An Appraisal of viscous oil–water two-phase flow through an undulated pipeline in peak configuration

ARTICLE *in* EXPERIMENTAL THERMAL AND FLUID SCIENCE · APRIL 2015

Impact Factor: 1.99 · DOI: 10.1016/j.expthermflusci.2015.04.017

3 AUTHORS:

Anand Babu Desamala

National Institute of Technology, Warangal

9 PUBLICATIONS **10** CITATIONS

SEE PROFILE

Ashok Kumar Dasmahapatra

Indian Institute of Technology Guwahati

26 PUBLICATIONS **50** CITATIONS

SEE PROFILE

Tapas K. Mandal

Indian Institute of Technology Guwahati

35 PUBLICATIONS **146** CITATIONS

SEE PROFILE

Experimental Thermal and Fluid Science 68 (2015) 177–186

Contents lists available at ScienceDirect

Experimental Thermal and Fluid Science

journal homepage: www.elsevier.com/locate/etfs

An appraisal of viscous oil–water two-phase flow through an undulated pipeline in peak configuration

Anand B. Desamala, Ashok Kumar Dasmahapatra *, Tapas K. Mandal [1]

Department of Chemical Engineering, Indian Institute of Technology Guwahati, Guwahati, Assam 781039, India

ARTICLE INFO

Article history:
Received 27 July 2014
Received in revised form 25 February 2015
Accepted 16 April 2015
Available online 24 April 2015

Keywords:
Undulated pipeline
Viscous oil–water flow
Flow pattern transitions
Wispy annular flow
Electrical conductance probe

ABSTRACT

Experimental results on flow patterns and pressure drop characteristics of viscous oil–water flow through undulated pipeline in peak configuration have been studied in this work. Undulated pipeline consists of two inclined sections (uphill and downhill) connected between two horizontal pipes (upstream and downstream) at peak configuration. Experiments have been conducted over a wide range of superficial velocities of oil (U_{SO} = 0.015–1.3 m/s) and water (U_{SW} = 0.1–1.2 m/s). Seven different flow patterns (viz., plug, slug, wavy stratified, stratified mixed, wispy annular, dispersion of oil in water and dispersion of water in oil) are identified by visual, imaging and electrical conductance probe techniques at all the four sections. Our results shows that present undulation (5°) has a marginal effect on the flow behavior of viscous oil–water mixture and the range of fluid velocity differs for a particular flow pattern. The pressure gradient characteristics across the peak experiences relatively more pressure gradient as compared to upstream and downstream at $U_{SW} \geqslant 0.6$ m/s, which is attributed to the combined effect of undulation (viz., peak configuration) along the pipeline, flow pattern, and effective viscosity and density of the fluid mixture.

1. Introduction

The flow of two immiscible liquids occurs commonly in petroleum industry, where crude oil and water produced from wells, are transported over long distances for subsequent separation and processing. In such cases, undulation of pipelines comprising of interconnected horizontal, upward and downward inclined sections are inevitable due to different elevation of the earth surface. Therefore, it is necessary to understand the different flow patterns and their transition boundaries for proper designing and sizing of a downstream separation and other unit of processing facilities. Flow patterns are the different interfacial distribution among themselves during the flow of two immiscible fluids through pipelines. There are several flow patterns reported in the literature: Slug (S), Plug (P) Stratified wavy (SW), Stratified mixed (SM), Annular (A), Dispersion of oil in water ($D_{O/W}$) and Dispersion of water in oil ($D_{W/O}$). Plug flow (P) is observed at low flow rate of both the fluid, with the appearance of small discrete oil droplets in continuous water phase. This plug flow becomes slug flow (S) when length of oil plugs is comparable with pipe diameter. In stratified wavy (SW), two phases (say oil and water) are separated as two continuous layers with a clear and wavy interface. Sometimes small oil droplets appear at interface and this layer is sandwiched between continuous oil (on top) and water (bottom) layer. This pattern is known as stratified mixed flow (SM). In annular (A) flow pattern, oil flows at the center of the tube as a continuous core and the water flows as an annulus. At higher phase velocities, one phase dispersed into another continuous phase. Depending upon the dispersed phase and continuous phase it is termed as dispersion of oil in water ($D_{O/W}$), dispersion of oil in water and water ($D_{O/W\&W}$), dispersion of water in oil ($D_{W/O}$), dispersion of water in oil and oil ($D_{W/O\&O}$). An overview of reported literature work on liquid–liquid two-phase flow is presented below.

Various experimental works have been performed in literature to enhance the understanding of liquid–liquid flow since 1950. Clark and Shapiro [1] in their pioneering work have developed a method of transportation of viscous oil by injecting small amount of water to reduce pressure drop during flow. Russell et al. [2] proposed a classification of the observed flow patterns in horizontal pipeline after conducting a series of experiments systematically on oil–water flow. In 1960s and 1970s, most of the researchers mainly focused on improving pumping requirements during viscous oil transportation by introducing water in the pipeline [3,4]. In recent years, hydrodynamics (in particular on flow patterns

* Corresponding author. Tel.: +91 361 2582273; fax: +91 361 2582291.
E-mail addresses: akdm@iitg.ernet.in (A.K. Dasmahapatra), tapasche@iitg.ernet.in (T.K. Mandal).
[1] Tel.: +91 361 2582271; fax: +91 361 2582291.

http://dx.doi.org/10.1016/j.expthermflusci.2015.04.017
0894-1777/

Nomenclature

A	wispy annular flow
$D_{O/W\&W}$	dispersion of oil-in-water and water flow
$D_{O/W}$	dispersion of oil in water flow
$D_{W/O}$	dispersion of water in oil flow
LED	Light Emitting Diode
P	plug flow
S	slug flow
SM	stratified mixed flow
SW	stratified wavy flow
TL	three layer flow
TS	test section
U_{SO}	oil superficial velocity (m/s)
U_{SW}	water superficial velocity (m/s)

and transition characteristics) of oil–water two-phase flow have received considerable attention by various researchers [5–21]. Lum et al. [5] have investigated the effect of upward (+5°, +10°) and downward (−5°) pipe inclinations on flow patterns, holdup and pressure gradient during oil–water flows at mixture velocity, 0.7–2.5 m/s. It has been observed that the frictional pressure gradient in both upward and downward flow is lower than that of horizontal flow. The frictional pressure drop becomes minimum for all inclinations at high mixture velocities, where transition from dispersed water-in-oil to dual continuous flow takes place. A comprehensive review on oil–water flow patterns in horizontal pipe can be found in Trallero et al. [9]. Rodriguez and Oliemans [6] have reported experimental results on oil–water flow in different pipe inclinations (−5°, −2°, −1.5°, 0°, 1°, 2° and 5°), and observed a stable wavy flow in downward inclined pipe and higher water recirculation in upward inclined pipes. They have also observed that stratified smooth flow disappears and replaced by stratified wavy flow. The stability of a particular flow pattern depends on the balance between various forces. For example, Ooms et al. [22] have shown that the balance between the hydrodynamic force and buoyancy force on the core establishes an eccentric core annular flow in a horizontal pipe. Core annular flow among the all is more significant because of low pressure drop and hence, minimum pumping power is needed for transportation of oil. This core-annular configuration is attained when viscous oil phase is surrounded by water annulus [23–30].

Much attention has been given in understanding flow behavior of oil–water system in horizontal and vertical pipeline. Flow patterns in undulated pipeline with inter-connected horizontal, inclined downward and upward section are not well understood. A limited number of studies have focused to understand the liquid–liquid [31,32] and air-oil-water [33] flow in undulated pipeline. Abduvayt et al. [31] have investigated flow pattern, pressure drop and water holdup in hilly terrain pipeline for oil–water (oil viscosity = 1.88 ± 0.19 mPa s) flow. They have also observed that the stratified smooth flow was totally absent at +3° uphill and −3° downhill sections of the hilly terrain pipeline. They also noted that the range of dual continuous pattern reduces compared to the horizontal one (by visual and video recording). Mandal [32] have estimated the flow patterns of oil–water flow (oil viscosity = 1.2 mPa s) by using probe signal analysis in an undulated pipeline in peak configuration. He has observed that transition boundaries of stratified wavy to three-layer flow and three layer to dispersed flow vary from section to section of peak configuration. However, it is same for plug/slug flow at different sections. CFD simulation as complementary to the experimental results has also been carried out by various authors for both gas–liquid [34–37] and liquid–liquid [38–43]) flow.

Although the hydrodynamics of low viscous oil–water flow in hilly terrain and undulated pipeline has been studied, the flow behavior of moderately viscous oil–water flow is poorly understood. Hilly terrain and undulation of pipeline is a more realistic situation for a transportation pipeline. In this work, the aim has been triggered on the effect of undulation (viz., peak configuration with an angle of 5°) on the hydrodynamics of moderately viscous oil–water flow (oil viscosity = 107 mPa s). Crude oil with viscosity ⩾ 100 mPa s is quite relevant to oil refineries in coming years [26,27,44]. Most of the reported results are based on low inclination [31,32], therefore, the angle of inclination in our study is selected as 5° for comparative analysis with the literature. It is found that the small undulation does not have too much effect on flow pattern, except shifting the flow pattern transition to different superficial velocities of oil and water.

2. Experimentation

2.1. Description of the setup

The schematic diagram of the experimental setup is shown in Fig. 1. It consists of 7.4 m long transparent Perspex (PMMA) pipe with 0.025 m internal diameter. It consists of an entry section (EN), a test section (TS) and an exit section (EX) in order of the direction of flow. The exit section is connected with the separator (S1). In the test sections, view boxes (VB1 to VB4) are provided to minimize the lens effect of the pipe material during the photography. Water and lube oil are selected as test fluids and the physical properties are presented in Table 1. Interfacial tension is measured using a plate type tensiometer (Make: KRUSS, Germany; Model: K9) and viscosity is measured by a rheometer (Haake Rheo Stress 1; Make: Thermo Electron Corporation, Germany; Model: RS. −1). Water and oil are pumped by a centrifugal (CP) and a gear pump (GP) respectively. A pair of pre-calibrated rotameters (RM1 and RM2) ranging from (0–1.67×10^{-4} m^3/s) for RM1 and (0–9.17×10^{-4} m^3/s) for RM2 measure water flow rates. The oil flow rate (7.4×10^{-6}–6.1×10^{-4} m^3/s) is measured by volumetric method due to lack of sophisticated instrumentation. In this process, oil volumetric flow rate is obtained by the subtraction of water volumetric flow rate (obtained from precalibrated rotameter) from mixture (total) volumetric flow rate of oil–water mixture. Mixture volumetric flow rate (total volumetric flow rate) is measured by finding out total liquid height of the mixture present in the calibrated decanter at the exit and the time required for reaching a particular liquid level. Latter on the oil flow rate obtained from this method is calibrated with help of a pre-calibrated Micro Motion Coriolis mass flow meter (Make: Emerson Process Management, Sensor Model: R100S128NQBZEZZZZ, Transmitter Model: 1700R11ABFEZZZ) when it was available. The calibration plot is plotted in Annexure (Fig. A1), which shows a good correlation coefficient (R^2 = 0.99).

To avoid any temperature effect on the physical properties of fluids during the experiment, the experiment has been run for around 15 min and stopped for around 1.5 h (for separating oil from oil–water mixture). The experiments have been repeated thrice to check the reproducibility of volumetric flow rate and a good reproducibility has been observed with an average deviation

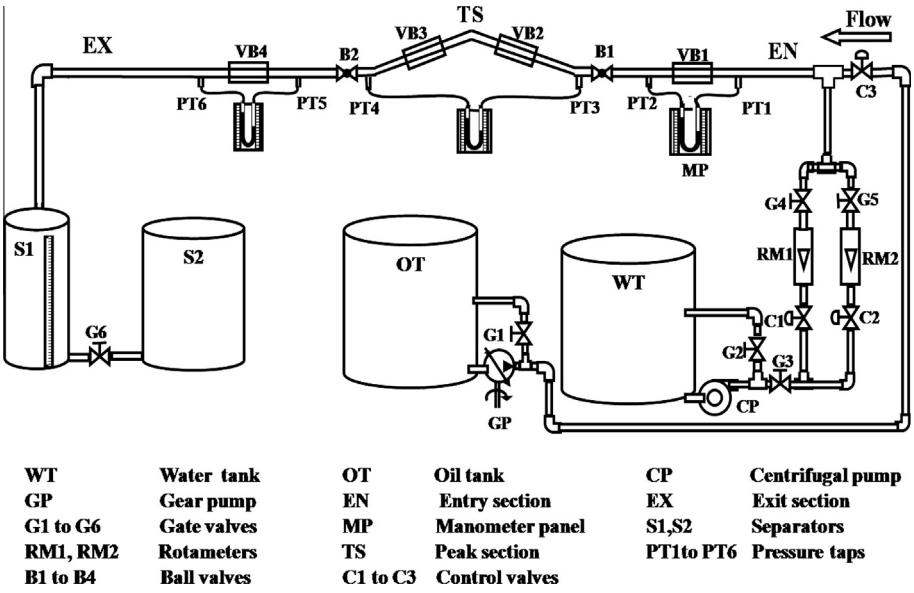

Fig. 1. Schematic representation of experimental setup.

Table 1
Physical properties of test fluids.

Properties	Fluids	
	Water	Oil (SAE 40)
Density (kg/m^3)	1000	890
Viscosity (Pa s)	0.001	0.107
Surface tension (N/m)	0.072	0.032
Interfacial tension (oil-water) (N/m)	0.024	

of 0.5%. Uncertainty in measurement of volumetric flow rate is also calculated and it is found around in the order of 10^{-4}.

Fig. 2 shows the detailed dimensions of the test sections. Test section of peak configuration comprises of an uphill (UH) and a downhill section (DH) between two horizontal portions (upstream (US) and downstream (DS) section) in order of the direction of flow. The junction of the upstream and uphill section is termed as the uphill elbow and that between the downhill and downstream section is the downhill elbow. The angle of inclination is equal for both the uphill and downhill sections with ±5° with respect to the horizontal.

2.2. Experimental procedure

Experiments have been performed at a particular oil and water velocity. In steady state, a snapshot has been taken using a digital camera (Make-SONY, Model-DSC HX100V) at all test sections to identify the flow pattern. A U-tube manometer (with CCl_4 as manometric fluid) is used to determine the pressure difference across the undulated section. This experiment has been repeated three times to check the reproducibility of the experimental results. More than 99% reproducibility has been obtained in most of the cases. After completion of a set of experiments, oil velocity is increased step-by-step (by gradual opening the control valve C3), keeping the water velocity constant and readings are repeated as earlier. Likewise, the experiments are completed for entire range of velocities.

2.2.1. Electrical conductance probe

The most common way to identify the interfacial configuration is visual/video observations [45] and probe (intrusive and non-intrusive) techniques [46,47]. In the present work, an electrical conductance probe (intrusive) is used to identify the wispy annular flow (A) (other flow patterns have been identified by photographic technique). During wispy annular flow, oil flows at the center of the tube as continuous core and water in contact with the pipe wall. A very thin layer of water flows as annulus in annular flow, which is difficult to identify visually, and by photography. Therefore, in the present work, an electrical conductance probe has been used to identify the annular flow. The position of probe at different section is shown in Fig. 2. The schematic representation of this probe and cross sectional view of flow configuration is shown in Fig. 3a and b respectively. It consists of two different

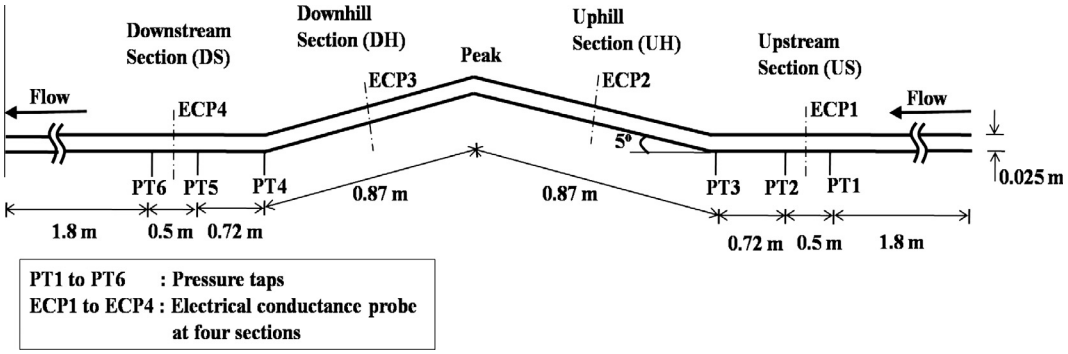

Fig. 2. Detailed dimensions of the test sections.

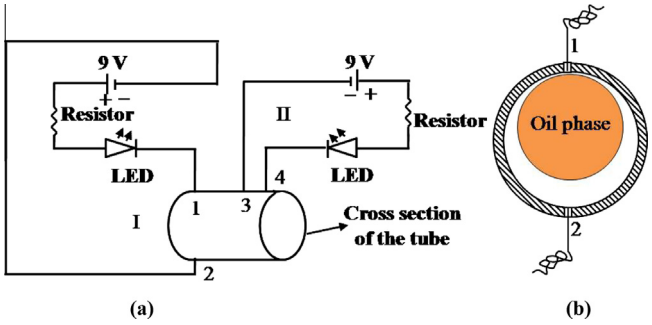

Fig. 3. Arrangement of conductance probe and phase configuration; (a) electrical conductance probe; (b) cross sectional view with phase configuration.

circuits: circuit-I and circuit-II. Each circuit is composed of two wires (1 and 2 in circuit-I; 3 and 4 in circuit-II) which acts as electrodes connected to an electrical circuit. The wires used for the probe are 0.35 mm thick. Electrodes 1 and 2 of circuit-I are placed diametrically opposite position on the pipe cross section, and 3 and 4 of circuit-II are placed 30 mm apart along the length on top of pipe wall. The electrical circuit consists of an LED, a resistor and a 9 V battery. In each circuit, one wire is connected directly to the cathode of the battery and other wire is connected to the short lead of the LED. Other lead of the LED is connected to one end of the resistor (250 Ohms) and other end is connected to anode of the battery (Fig. 3a). The circuit will be completed through 1–2 in circuit-I and 3–4 in circuit-II, if water present in between. This circuit is tested by running water and oil separately. LED in this circuit glows when only water is running in the pipe because water is a good conductor of electricity. When only oil is flowing, LED does not glow because oil is a very poor conductor of electricity. Glowing of LED's in both circuits confirms the existence of water layer in annulus position and it confirms the existence of annular flow.

3. Results and discussion

The experiments have been conducted for a wide range of superficial velocity of oil and water (U_{SO} = 0.015–1.3 m/s) and (U_{SW} = 0.1–1.2 m/s) respectively, to cover the entire range of flow patterns. Flow patterns except wispy annular are identified by imaging technique and wispy annular flow is identified using both probe and imaging technique.

3.1. Identification of wispy annular flow and comparison with literature

Wispy annular flow is first identified by Hawkes and Hewitt [48]. In wispy annular flow, the structures are actually quite difficult to observe visually because the thin water film (especially on top region of oil core in horizontal flow) tends to be highly disturbed due to the presence of "disturbance waves". Sometimes the wave crest may touch upon the pipe wall. In the present study, wispy annular flow has been identified by probe and photographic technique as discussed in the experimental section. The result of this technique at U_{SW} = 0.4 m/s is summarized in Table 2 for upstream section. Top view, front view and a sketch of the cross sectional view of the flow pattern are shown in 4th, 5th and 6th column of the table respectively. Status of LED at particular flow rate is mentioned in 7th column, and over all remark is given in 8th column. At U_{SW} = 0.4 m/s and U_{SO} = 0.33 m/s, top (4th column) and front view (5th column) shows that water warps the core oil phase. The oil droplet entrainment into the water layer is also clearly noticed (Sl. No. 1 of Table 2). All the LEDs in circuit-I and II, are glowing at the same flow condition. It proves the occurrence of wispy annular flow pattern at this phase flow rate. Similarly, this flow pattern is identified at other velocities as mentioned in Sl. No. 2 and 3 of Table 2. By increasing the oil velocity from 0.33 m/s to 0.685 m/s, droplet entrainment in water layer increases as in Sl. No. 2 and 3 of Table 2. Further increasing the oil velocity, dispersion of water in oil flow pattern is observed and LED is not glowing further.

The wispy annular flow region is observed at U_{SO} = 0.28–0.73 m/s and U_{SW} = 0.39–0.59 m/s for both upstream and uphill sections. For downhill and downstream sections the wispy annular flow is observed at U_{SO} = 0.25–0.73 m/s with the same water velocities (viz., U_{SW} = 0.39–0.59 m/s) (see Section 3.3 for flow pattern map). At lower velocities of oil and water, the wispy annular flow is not stable because of capillary instability (due to interfacial tension) and it breaks the oil core [23]. However, at higher velocity, interfacial frictional instability factor reduces the capillary

Table 2
Identification of wispy annular flow.

S. No.	U_{SW} (m/s)	U_{SO} (m/s)	Photograph of the flow		Cross sectional view	LED glowing	Flow pattern
			Top view	Front view			
1	0.4	0.33		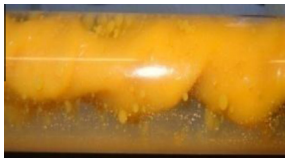		Yes	Wispy annular flow
2	0.4	0.50				Yes	Wispy annular flow
3	0.4	0.68		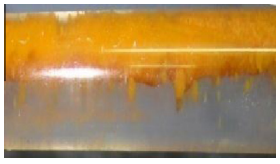		Yes	Wispy annular flow

instability and stabilizes the wispy annular flow. For higher velocities, wispy annular flow becomes again unstable due to the domination of the interfacial friction, which breaks the core. The wispy annular flow observed in present experimental condition has been compared with the literature data of annular flow in Table 3. The table shows the viscosity of oil used in the present work is less than the others except Charles et al. [3]. Pipe diameter is also comparable with all the works except Poesio et al. [27]. The velocity range of wispy annular flow observed in the present study lies within the ranges reported in the past literature (Table 3) but the magnitude of the range is less in present work. This is due to the destabilizing effect of peak configuration. Poesio et al. [27] and Sotgia et al. [25] work shows that larger diameter destabilizes the annular flow. Sotgia et al. [25] and Grassi et al. [24] also concluded that the stability of the annular flow depends on the pipe geometry, operating conditions, viscosity and density of the liquids used in the system.

3.2. Different flow patterns

Seven different flow patterns are observed at each section during oil–water flow through peak configuration of the undulated pipeline. Those are plug flow (P), slug flow (S), stratified wavy flow (SW), stratified mixed flow (SM), wispy annular flow (A) (see Section 3.1 for details), dispersion of oil in water flow ($D_{O/W}$) and dispersion of water in oil flow ($D_{W/O}$). The representative photographs of different observed flow patterns in peak configuration are shown in Fig. 4. There is no significant influence of this small undulation (undulation is 5°, see Fig. 2 for detailed dimensions of the set up) on the flow patterns at four different sections. Several forces, such as, inertial, surface, buoyancy, viscous and gravity, govern stability of a particular flow pattern. At low oil and water velocity (U_{SW} = 0.13–0.59 m/s and U_{SO} = 0.017–0.28 m/s), surface, buoyancy and gravity forces dominate over inertial and viscous forces. As a result, shape of oil slug nose (Fig. 4a and b) and interfacial waves (Fig. 4c) vary along the pipeline. Droplet concentration at the interface of stratified mixed flow (Fig. 4d) varies across the sections, where viscous, buoyancy and gravity dominate over others. It is also observe that the shape of the lower interfacial wave in wispy annular flow is also changing from section to section (Fig. 4e). Concentration of oil droplet in dispersion of oil in water ($D_{O/W}$) is more at the downstream section starting from the end of downhill section (Fig. 4f). At this section, gravity facilitates the water phase (heavier) to move faster than the oil phase (lighter) and increases the slippage between the phases. As a result, oil droplet concentration increases. Dispersion of water in oil ($D_{W/O}$) flow (Fig. 4g) is observed at higher oil velocity (U_{SO} = 0.8 m/s).

3.3. Flow pattern maps at different sections and a comparison among them

The observed flow patterns at four different sections (upstream, uphill, downhill and downstream) of the undulated pipeline are presented in the form of flow pattern maps (Fig. 5a–d respectively). The superficial velocities of oil (U_{SO}) and water (U_{SW}) are selected as coordinate axes of the plots. Scattered points in Fig. 5 represent different flow patterns observed at different phase velocities. Fig. 5a–d depicts same flow patterns at each section differing in velocity ranges. For a better understanding, four flow pattern maps for four different sections are superimposed on each other in Fig. 6 to understand the effect of undulation on flow patterns.

In the Fig. 6, solid black color line shows the transitions at upstream section, dotted blue color line shows the transitions at uphill section, red color dash dot line shows the transitions at downhill section and green color dashed line shows the transitions observed at downstream section. The salient features of the observations are described below.

- The transition boundaries of P to S, S to SW, SW to SM and SM to A are almost identical at all the four sections.
- A small variation is observed in the transition of slug to annular flow at upstream and uphill section. Slug flow occupies a larger area in upstream and uphill section as compared to the other sections. Uphill elbow at peak configuration decelerate the velocity at uphill section [49], where, surface force dominates over other forces. As a result, and annular flow breaks up into large slugs giving rise to slug flow.
- Similar deviations are also observed for the transition boundaries of $D_{O/W}$ to SM at upstream and uphill sections. However, $D_{O/W}$ flow is observed at higher oil velocity at these two sections.
- SM to $D_{W/O}$ and A to $D_{W/O}$ flow transition is observed at higher oil velocities at uphill section. Flow direction changes form horizontal to upward inclination at uphill section, where gravity retards the flow and reduces the wave amplitude causing the onset of $D_{W/O}$ at higher velocity.

From the above discussion, it appears that the influence of undulation on flow patterns is reasonably small.

3.4. Effect of viscosity on flow pattern in undulated pipeline

To understand the effect of viscosity on the flow patterns, the present work is compared with the flow pattern maps given by Mandal [32] for peak configuration. Pipe material, pipe diameter and pipe inclination used in the present study is same as Mandal [32]. The only difference is in the physical properties of oil. Oil viscosity is almost 90 times higher than that of Mandal [32]. Fig. 7 shows the comparison between these two flow pattern maps at upstream section. In figure, the scattered data points show the experimental results and solid black line shows the flow transitions boundaries observed by Mandal [32]. Dispersion of oil-in-water and water ($D_{O/W\&W}$) and three layer (TL) flow of Mandal [32] are considered as dispersion of oil in water ($D_{O/W}$) and stratified mixed flow (SM) respectively in the present work to avoid the complexity in nomenclature of different flow patterns. The salient differences are as follows.

Table 3
Comparison of annular flow velocity: Experimental results with literature data.

Author	System	Pipe diameter (cm)	Core fluid viscosity (kg/ms)	Velocity range of core fluid (m/s)	Velocity range of water (m/s)
Charles et al. [3]	Horizontal	2.5	0.0063, 0.0168, 0.065	0.015–0.9	0.03–1.07
Grassi et al. [24]	Horizontal, upward downward	2.1	0.799	0.186–0.7	0.15–1.95
Sotgia et al. [25]	Horizontal	2.6	0.9	0.28–0.97	0.16–1.73
Pietro Poesio et al. [27]	Horizontal	5.0	0.9	0.25–0.48	0.3–0.55
Present work	Upstream	2.5	0.107	0.28–0.73	0.40–0.60
	Uphill			0.28–0.73	
	Downhill			0.25–0.73	
	Downstream			0.25–0.73	

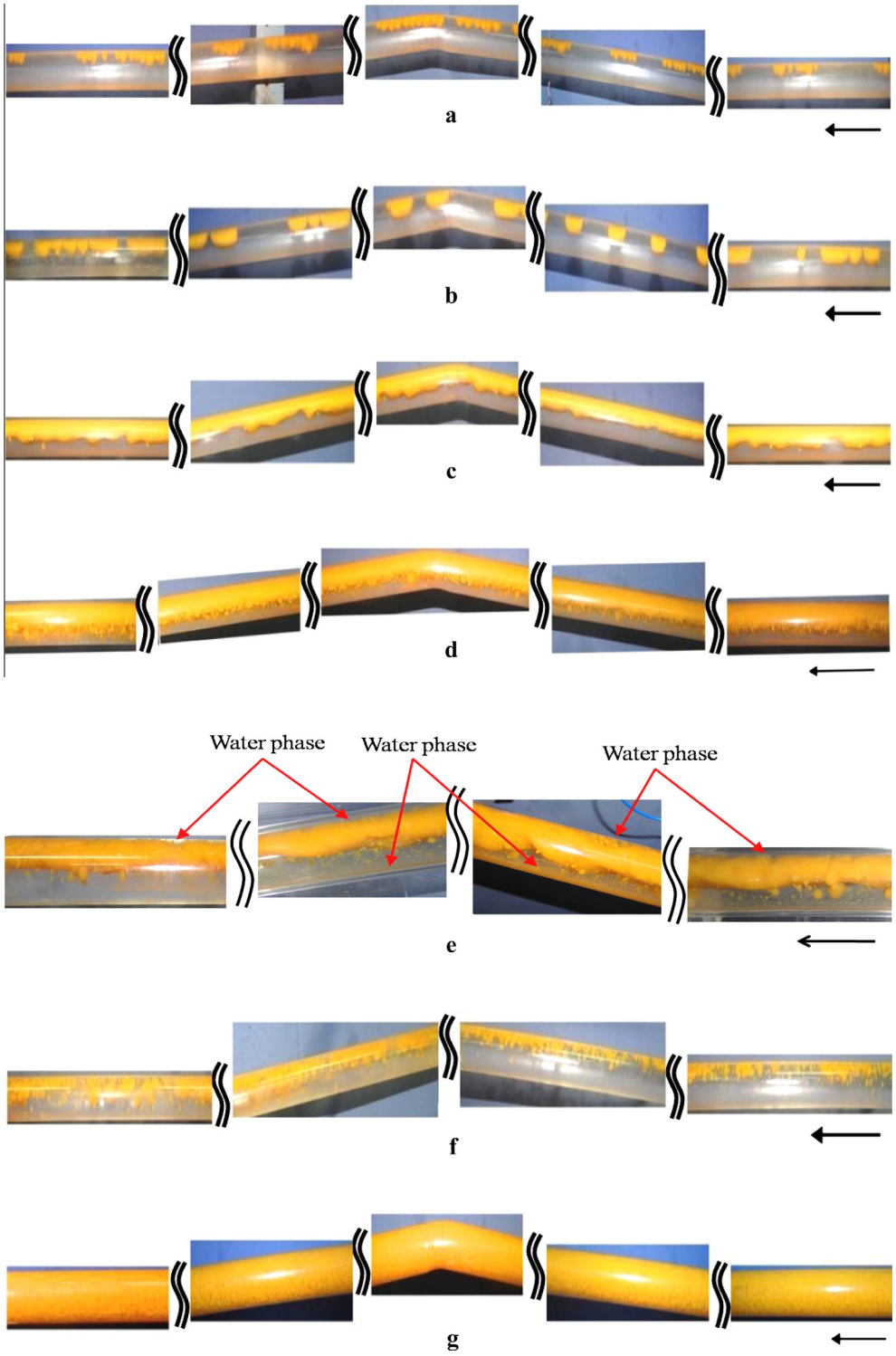

Fig. 4. Experimental images of observed flow patterns; (a) plug flow (P) at U_{SO} = 0.032 m/s, U_{SW} = 0.3 m/s; (b) slug flow (S) at U_{SO} = 0.061 m/s, U_{SW} = 0.23 m/s; (c) stratified wavy flow (SW) at U_{SO} = 0.165 m/s, U_{SW} = 0.165 m/s; (d) stratified mixed flow (SM) at U_{SO} = 0.42 m/s, U_{SW} = 0.2 m/s; (e) wispy annular flow (A) at U_{SO} = 0.48 m/s, U_{SW} = 0.5 m/s; (f) dispersion of oil in water flow ($D_{O/W}$) at U_{SO} = 0.21 m/s, U_{SW} = 0.70 m/s; (g) dispersion of water in oil flow ($D_{W/O}$) at U_{SO} = 0.84 m/s, U_{SW} = 0.40 m/s.

- Slug and Wispy annular flow observed in present work those are not reported by Mandal [32] because high viscosity favors all these flow. Russell et al. [2] and Grassi et al. [24] also observed similar phenomena in horizontal flow. Plug and stratified mixed flow observed at lower water velocities (0.1 m/s) and occupy larger area of the flow pattern map in the present work (U_{SW} = 0.1–1.15 m/s and U_{SO} = 0.2–0.76 m/s) as compared to his work (U_{SW} = 0.2–0.48 m/s and U_{SO} = 0.12–0.7 m/s). Balakhrisna et al. [26] also reported wide velocity span of such flow at downstream section of a sudden expansion/contraction in a horizontal pipeline. They used a viscous oil having viscosity of 200 mPa s. It happens because higher viscosity of the fluid

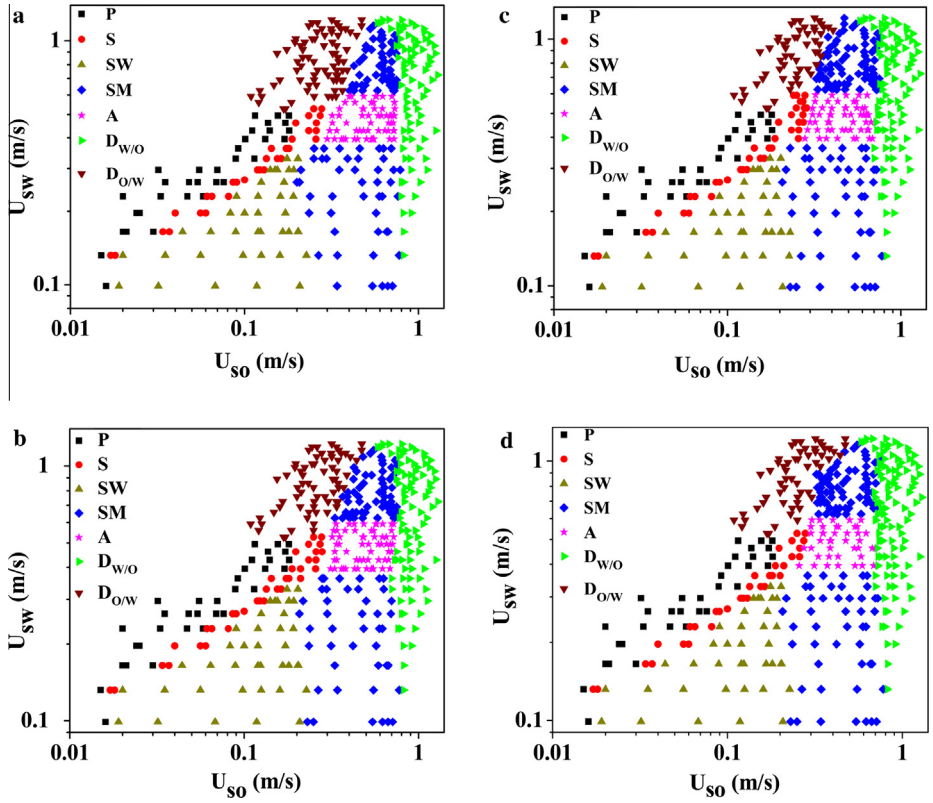

Fig. 5. Observed flow pattern maps. (a) Upstream section; (b) uphill section; (c) downhill section; (d) downstream section. (P – Plug flow, S – Slug flow, SW – Stratified wavy flow, SM – Stratified mixed flow, A – Wispy annular flow, $D_{W/O}$ – Dispersion of water in oil flow, $D_{O/W}$ – Dispersion of oil in water flow).

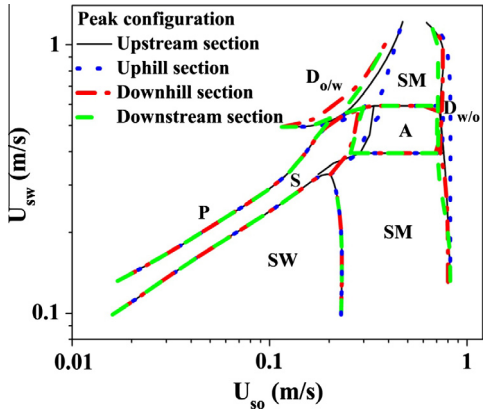

Fig. 6. Comparison of flow pattern maps observed at upstream, uphill, downhill and downstream sections (P – Plug flow, S – Slug flow, SW – Stratified wavy flow, SM – Stratified mixed flow, A – Wispy annular flow, $D_{W/O}$ – Dispersion of water in oil flow, $D_{O/W}$ – Dispersion of oil in water flow).

increases the friction and drag coefficients and favors the formation of droplets at the interface by overcoming the surface force.

- Velocity range of stratified wavy (U_{SW} = 0.035–0.28 m/s and U_{SO} = 0.05–0.7 m/s) and dispersion of oil in water flow (U_{SW} = 0.292–0.68 m/s and U_{SO} = 0.02–0.7 m/s) in his work is larger than the present work (U_{SW} = 0.1–0.33 m/s, U_{SO} = 0.02–0.23 m/s for SW and U_{SW} = 0.52–1.22 m/s, U_{SO} = 0.11–0.47 m/s for $D_{O/W}$). His $D_{O/W}$ flow is shared by plug, slug, stratified mixed and wispy annular flow pattern in the present work. Mandal [32] and Rodriguez and Oliemans [6] works show the larger velocity span of stratified wavy flow for low viscous oil, having viscosity = 1.2 mPa s and 7.17 mPa s respectively in horizontal pipeline. Dispersion of oil in water starts at higher phase velocities in the present work. The present work has also been compared with Mandal [32] at other three sections, and found the differences are quite similar as discussed above, except minor deviation in velocity ranges for different flow patterns.

4. Effect of undulation (peak configuration) on pressure gradient

A comparison of total pressure gradient at the upstream (PT1–PT2), across peak (i.e. combination of uphill and downhill sections, PT3–PT4) and downstream (PT5–PT6) section of peak configuration at different constant water velocities (U_{SW} = 0.2, 0.4, 0.6, 1.0 m/s) have been plotted in Fig. 8. The distance between the

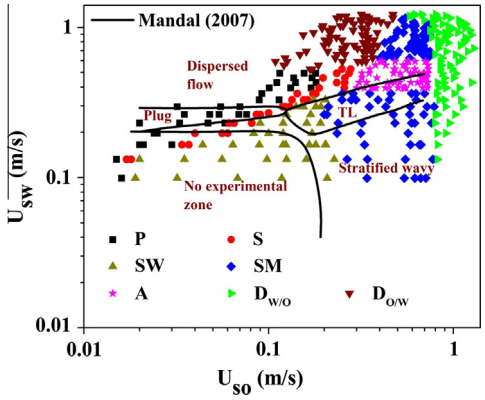

Fig. 7. Comparison of upstream flow pattern map with Mandal [32] (P – Plug flow, S – Slug flow, SW – Stratified wavy flow, SM – Stratified mixed flow, A – Wispy annular flow, $D_{W/O}$ – Dispersion of water in oil flow, $D_{O/W}$ – Dispersion of oil in water flow).

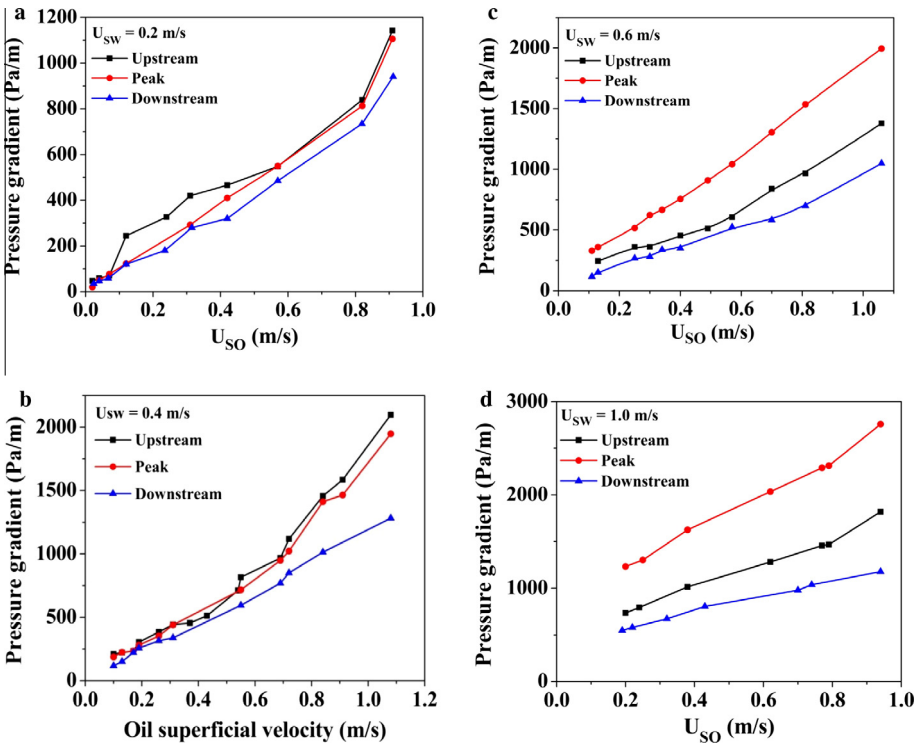

Fig. 8. Variation of pressure gradient with increase in oil and water velocities; (a) U_{SW} = 0.2 m/s; (b) U_{SW} = 0.4 m/s; (c) U_{SW} = 0.6 m/s; (d) U_{SW} = 1.0 m/s.

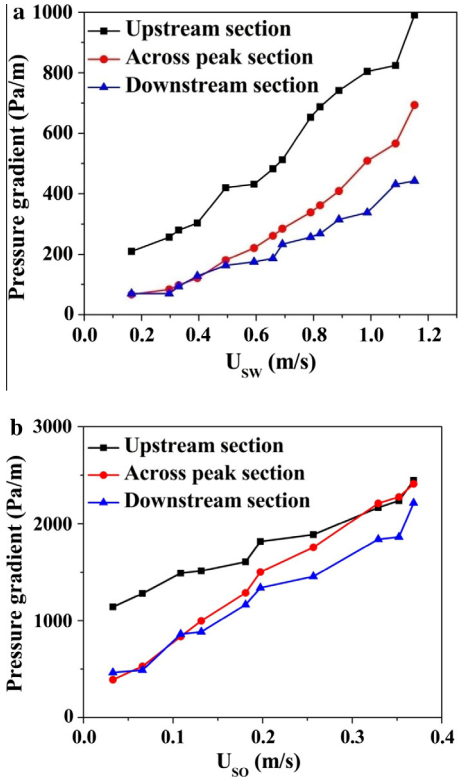

Fig. 9. Pressure gradient for single-phase flow; (a) water only flow; (b) oil only flow.

pressure taps of upstream (PT1–PT2), across peak (PT3–PT4) and downstream (PT5–PT6) section are 0.5 m, 1.74 m and 0.5 m respectively as shown in Fig. 2. This actual distance across the peak is used to get total pressure gradient from the pressure drop data. Fig. 8a–d depicts that, pressure gradient at three sections increases with increasing the oil velocity for all the cases. The pressure gradient in three different sections of peak configuration are comparable (Fig. 8a and b) at low water flow rate (U_{SW} = 0.2 and 0.4 m/s). At these water flow rates, pressure gradient decreases from upstream to downstream section. This trend is very similar with single-phase pressure drop (water or oil only values) as shown in Fig. 9a and b. The pressure gradient of three different sections in peak does not remain comparable at $U_{SW} \geqslant 0.6$ m/s (Fig. 8c and d) and not following the same trend observed at lower velocities. It is also in disagreement with the trend obtained for single-phase flow (Fig. 9a and b). The pressure gradient is maximum across a peak as shown in Fig. 8c and d. This trend (viz., non-monotonic trend in pressure gradient of upstream, peak and downstream section) has also been observed by Abduvayt et al. [31] in their experimental work on hilly terrain pipeline. Although the exact reason is not well understood, however this non-monotonic trend in pressure gradient may be due to the combined effect of inclination, slip and effective density arises during flow. At high water velocity (viz., $U_{SW} \geqslant 0.6$ m/s), dispersed flow pattern appears, which influences the effective density and viscosity of the fluid mixture. Pressure gradient is a strong function of effective viscosity of the phase mixture. The effective viscosity also depends on degree of heterogeneity of the phases, which results from the degree of dispersion of a secondary phase. Uphill elbow and peak distribute the oil droplets more uniformly across the pipe cross section at these higher velocities, which enhance the effective viscosity and pressure gradient. Slip during flow is also playing an important role in influencing pressure gradient. Slip is more in case of upward flow compared to downward flow [31], and as a result, oil fraction is more at downhill section which increase the pressure gradient across the peak. For these two reasons, net pressure gradient across the peak increases as shown in Figs. 8c, and d.

It appears from trend in Figs. 8 and 9 that pressure drop is influenced by the undulation (viz. peak) along the flow path and the fluid velocity. Upstream section because of the presence of peak ahead of it, experiences more pressure drop than the downstream section. Flow is slightly accelerated in downstream and

decelerated in upstream section (gravity plays a role too) due to the presence of a peak. Therefore, upstream pressure gradient is more than the downstream pressure gradient. On the other hand, the effect of peak is more pronounced at low fluid velocity, than at high velocity. Therefore, the pressure gradient at high velocity across peak is almost same as the upstream section. At low velocity, downstream elbow dominates over peak and as result, pressure gradient at downstream section is close to that of the value across the peak. The observed pressure drop trend (Fig. 9) for single-phase fluid flow is distinctly different from the horizontal pipe flow, which is attributed to the presence of a peak with two numbers of elbow.

5. Conclusion

The experimental work has been carried out to understand the effect of undulation on the hydrodynamics of viscous oil–water flow. A peak configuration (with ±5° inclination) has been selected to represent a single unit of undulation in the pipeline. Seven different flow patterns (viz., plug flow, slug flow, stratified wavy flow, stratified mixed flow, wispy annular flow, dispersion of oil in water flow and dispersion of water in oil flow) have been observed at all the four sections. These flow patterns of all four sections are presented in the form of flow pattern maps, and compared with each other. Comparison across the sections shows that small undulation (5°) has a marginal effect on the flow behavior of viscous oil–water mixture. All the flow patterns have been observed in all the cases; however, the range of fluid velocity differs for a particular flow pattern. The velocity span of wispy annular flow obtained in the present study is comparable with the reported literature data. Present work deals with moderately viscous oil. Comparison of the present results with the work by Mandal [32] for low viscous oil shows that higher viscosity favors wispy annular, slug and dispersion of water in oil flow pattern. The pressure gradient data indicates that it is more across a peak at $U_{SW} \geqslant 0.6$ m/s due to the effect of undulation along the flow path. The understanding on the effect of undulation on the hydrodynamics of moderately viscous oil–water two-phase flow would be helpful in industrial design such as, pipe network for oil transportation.

Appendix A. Appendix

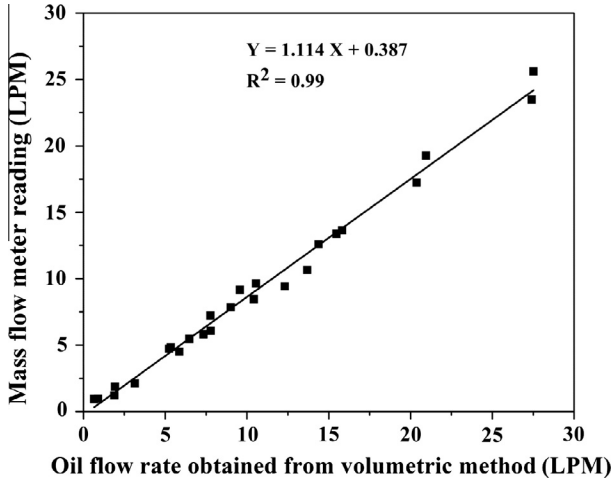

Fig. A1. Calibration curve of oil flow rate.

References

[1] A.F. Clark, A. Shapiro, U.S. patent No. 2, 533 (1949) 878.
[2] T.W.F. Russell, G.W. Hodgson, G.W. Govier, Horizontal pipeline flow of mixtures of oil and water, Can. J. Chem. Eng. 37 (1959) 9–17.
[3] M.E. Charles, G.W. Govier, G.W. Hodgson, The horizontal flow of equal density oil–water mixtures, Can. J. Chem. Eng. 39 (1961) 27–36.
[4] D. Hasson, U. Mann, A. Nir, Annular flow of two immiscible liquids: I mechanisms, Can. J. Chem. Eng. 48 (1970) 514–520.
[5] J.Y.-L. Lum, T. Al-Wahaibi, P. Angeli, Upward and downward inclination oil–water flows, Int. J. Multiphase Flow 32 (2006) 413–435.
[6] O.M.H. Rodriguez, R.V.A. Oliemans, Experimental study on oil–water flow in horizontal and slightly inclined pipes, Int. J. Multiphase Flow 32 (2006) 323–343.
[7] M. Nadler, D. Mewes, Flow induced emulsification in the flow of two immiscible liquids in horizontal pipes, Int. J. Multiphase Flow 23 (1997) 55–68.
[8] P. Angeli, G.F. Hewitt, Flow structure in horizontal oil–water flow, Int. J. Multiphase Flow 26 (2000) 1117–1140.
[9] J.L. Trallero, Cem Sarica, J.P. Brill, A study of oil/water flow patterns in horizontal pipes, SPE Prod. Facil. (SPE 36609), (1997) 165–172.
[10] D. Anjali, A.B. Desamala, A.K. Dasmahapatra, T.K. Mandal, Flow pattern of viscous oil–water flow: Prediction by probabilistic neural network (PNN) and validation with experimental data. In: Proceedings of 64th Annual Session of the IIChe, December 26–29, Bangalore, India, 2011.
[11] D. Anjali, A.B. Desamala, A.K. Dasmahapatra, T.K. Mandal, Correlation based pressure drop prediction of viscous oil–water two-phase flow through horizontal pipeline. In: Proceedings of 65th Annual Session of the IIChem, December 27–30, NIT Jalandhar, India, 2012.
[12] A.C. Bannwart, O.M.H. Rodriguez, C.H.M. de Carvalho, I.S. Wang, R.M.O. Vara, Flow patterns in heavy crude oil–water flow, ASME 126 (2004) 184–189.
[13] T.S. Raj, D.P. Chakrabarti, G. Das, Liquid–liquid stratified flow through horizontal conduits, Chem. Eng. Technol. 28 (2005) 899–907.
[14] M. Sharma, P. Ravi, S. Ghosh, G. Das, P.K. Das, Hydrodynamics of lube oil–water flow through 180° return bends, Chem. Eng. Sci. 66 (2011) 4468–4476.
[15] W. Wang, J. Gong, P. Angeli, Investigation on heavy crude-water two phase flow and related flow characteristics, Int. J. Multiphase flow 37 (2011) 1156–1164.
[16] N. Yusuf, Y. Al-Wahaibi, T. Al-Wahaibi, A. Al-Ajmi, S. Olawale, I.A. Mohammed, Effect of oil viscosity on the flow structure and pressure gradient in horizontal oil–water flow, Chem. Eng. Res. Des. 90 (2012) 1019–1030.
[17] G. Oddie, H. Shi, L.J. Durlofsky, K. Aziz, B. Pfeffer, J.A. Holmes, Experimental study of two and three phase flows in large diameter inclined pipes, Int. J. Multiphase Flow 29 (2003) 527–558.
[18] T. Fujii, J. Otha, T. Nakazawa, O. Morimoto, The behavior of an immiscible equal-density liquid–liquid two-phase flow in a horizontal tube, JSME Int. J. Series B 37 (1) (1994) 22–29.
[19] P. Angeli, G.F. Hewitt, Pressure gradient in horizontal liquid–liquid flows, Int. J. Multiphase Flow 24 (1998) 1183–1203.
[20] R. Manabe, H.Q. Zhang, E. Delle-Case, J.P. Brill, Crude oil-natural gas two-phase flow pattern transition boundaries at high pressure conditions. In: SPE Annual Technical Conference and Exhibition, Paper no. 71563, Louisiana, 2001.
[21] A. Dasari, A.B. Desamala, A.K. Dasmahapatra, T.K. Mandal, Experimental studies and PNN prediction on flow pattern of viscous oil–water flow through circular horizontal pipe, Ind. Eng. Chem. Res. 52 (2013) 7975–7985.
[22] G. Ooms, C. Vuik, P. Poesio, Core-annular flow through a horizontal pipe: Hydrodynamic counterbalancing of buoyancy force on core, Phys. Fluids 19 (2007) 1–17.
[23] A. Bensakhria, Y. Peysson, G. Antonini, Experimental study of the pipeline lubrication for heavy oil transport, Oil Gas Sci. Technol. -Rev. IFP 59 (2004) 523–533.
[24] B. Grassi, D. Strazza, P. Poesio, Experimental validation of theoretical models in two-phase high-viscosity ratio liquid–liquid flows in horizontal and slightly inclined pipes, Int. J. Multiphase Flow 34 (2008) 950–965.
[25] G. Sotgia, P. Tartarini, E. Stalio, Experimental analysis of flow regimes and pressure drop reduction in oil–water mixtures, Int. J. Multiphase Flow 34 (2008) 1161–1174.
[26] T. Balakhrisna, S. Ghosh, G. Das, P.K. Das, Oil–water flows through sudden contraction and expansion in a horizontal pipe – Phase distribution and pressure drop, Int. J. Multiphase Flow 36 (2010) 13–24.
[27] P. Poesio, D. Strazza, G. Sotgia, Two and three-phase mixtures of highly-viscous-oil/water/air in a 50 mm i.d. pipe, Appl. Therm. Eng. 49 (2012) 41–47.
[28] V.J.W. Parda, A.C. Bannwart, Modeling of vertical core-annular flows and application to heavy oil production, J. Energy Resour. Technol. ASME 123 (2001) 194–199.
[29] D. Strazza, B. Grassi, M. Demori, V. Ferrari, P. Poesio, Core-annular flow in horizontal and slightly inclined pipes: Existence, pressure drops, and hold-up, Chem. Eng. Sci. 66 (2011) 2853–2863.
[30] R.M. Mac Gillivray, K.S. Gabriel, Annular flow film characteristics in variable gravity, Ann. N. Y. Acad. Sci. 974 (2002) 306–315.
[31] P. Abduvayt, R. Manabe, T. Watanabe, N. Arihara, Analysis of oil/water-flow tests in horizontal, hilly terrain, and vertical pipes. SPE Prod. Oper. (SPE 90096), (2006) 123–133.
[32] T.K. Mandal, Some studies on Liquid–liquid slug flow. Ph.D. Thesis, IIT Kharagpur, India, 2007.

[33] S. Huang, B. Zhang, J. Lu, D. Wang, Study on flow pattern maps in hilly-terrain air–water–oil three-phase flows, Exp. Therm. Fluid Sci. 47 (2013) 158–171.
[34] A. Parvareh, M. Rahimi, A. Alizadehdakhel, A.A. Alsairafi, CFD and ERT investigations on two-phase flow regimes in vertical and horizontal tubes, Int. Commun. Heat Mass 37 (2010) 304–311.
[35] K. Ekambara, R.S. Sanders, K. Nandakumar, J.H. Masliyah, CFD simulation of bubbly two-phase flow in horizontal pipes, Chem. Eng. J. 144 (2008) 277–288.
[36] T. Frank, Numerical simulation of slug flow regime for an air–water two-phase flow in horizontal pipes. NURETH – 11, Oct 2–6, Popes' Palace conference center, France, 2005
[37] A. Huang, C. Christodoulou, D.D. Joseph, Friction factor and hold up studies for lubricated pipelining part-2: Laminar and k-ε models of eccentric core flow, Int. J. Multiphase flow 20 (1994) 481–491.
[38] T. Ko, H.G. Choi, R. Bai, D.D. Joseph, Finite element method simulation of turbulent wavy core-annular flows using a k-ε turbulence model method, Int. J. Multiphase Flow 28 (2002) 1205–1222.
[39] V.V.R. Kaushik, S. Ghosh, G. Das, P.K. Das, CFD simulation of core annular flow through sudden contraction and expansion, J. Pet. Sci. Eng. 86–87 (2012) 153–164.
[40] M.A. Al-Yaari, B.F. Abu-Sharkh, CFD prediction of stratified oil–water flow in a horizontal pipe, Asian Trans. Eng. 01 (2011) 68–75.
[41] S. Ghosh, G. Das, P.K. Das, Simulation of core annular downflow through CFD – A comprehensive study, Chem. Eng. Process. 49 (2010) 1222–1228.
[42] S. Ghosh, G. Das, P.K. Das, Simulation of core annular in return bends – A comprehensive CFD study, Chem. Eng. Res. Des. 89 (2011) 2244–2253.
[43] A.B. Desamala, D. Anjali, V. Vinayak, K.G. Bharath, A.K. Dasmahapatra, T.K. Mandal, CFD simulation and validation of flow pattern transition boundaries during moderately viscous oil–water two-phase flow through horizontal pipeline, Waset J. 73 (2013) 1150–1155.
[44] N.H. Abdurahman, Y.M. Rosli, N.H. Azhari, B.A. Hayder, Pipeline transportation of viscous crudes as concentrated oil-in-water emulsions, J. Petrol. Sci. Eng. 90–91 (2012) 139–144.
[45] T.K. Mandal, D.P. Chakrabarti, G. Das, Oil water flow through different diameter pipes similarities and differences, Chem. Eng. Res. Des. 85 (2007) 1123–1128.
[46] D.P. Chakrabarti, G. Das, P.K. Das, Identification of stratified liquid–liquid through horizontal pipes by a non-intrusive optical probe, Chem. Eng. Sci. 62 (2007) 1861–1876.
[47] T. Al-Wahaibi, P. Angeli, Experimental study on interfacial waves in stratified horizontal oil–water flow, Int. J. Multiphase Flow 37 (2011) 930–940.
[48] N.J. Hawkes, G.F. Hewitt, Experimental studies of wispy annular flow. Int. Symposium on Two-Phase Flow Modelling and Expt, 1995, 9–11.
[49] E. Al-Safran, C. Sarica, H.-Q. Zhang, J. Brill, Investigation of slug flow characteristics in the valley of a hilly-terrain pipeline, Int. J. Multiphase Flow 31 (2005) 337–357.